



# Hepatic and Intestinal Metabolism of Indinavir, an HIV Protease Inhibitor, in Rat and Human Microsomes

MAJOR ROLE OF CYP3A

Masato Chiba,\* Michelle Hensleigh and Jiunn H. Lin

DEPARTMENT OF DRUG METABOLISM, MERCK RESEARCH LABORATORIES, WEST POINT, PA 19486, U.S.A.

**ABSTRACT.** The metabolism of indinavir, a human immune deficiency virus (HIV) protease inhibitor, has been characterized extensively in rats and humans. All oxidative metabolites found *in vivo* were formed when indinavir was incubated with NADPH-fortified hepatic and intestinal microsomes obtained from rats and humans. *In vitro* kinetic studies revealed that  $V_{\max}/K_m$  values ( $\mu\text{L}/\text{min}/\text{mg}$  protein) in rat and human liver microsomes were approximately 8- and 2-fold greater than those in the intestinal microsomes of the corresponding species (55.8 and 6.7 for the liver and intestine, respectively, in rats; 16.5 and 7.7 for the liver and intestine, respectively, in humans). However, when  $V_{\max}/K_m$  was scaled up to intrinsic clearance ( $\text{mL}/\text{min}/\text{kg}$  body weight), hepatic intrinsic clearance was much greater than the intestinal clearance by 50- to 200-fold. These results suggest that the liver plays a much greater role in first-pass metabolism of indinavir than the intestine in both species. Consistently, ketoconazole, a selective inhibitor for CYP3A, and an anti-rat CYP3A1 antibody strongly inhibited hepatic and intestinal metabolism of indinavir in both rats and humans, suggesting the involvement of CYP3A isoforms in both organs. Oral treatment of rats with dexamethasone (50 mg/kg/day for 4 days), a potent CYP3A inducer, increased both hepatic and intestinal metabolism of indinavir by a factor of 7 and 3, respectively. Furthermore, indinavir selectively inhibited  $6\beta$ -hydroxylase activity of testosterone, a CYP3A marker activity, in rat and human liver microsomes; the interactions between testosterone and indinavir were competitive with  $K_i$  values of  $< 1.0 \mu\text{M}$ . BIOCHEM PHARMACOL 53;8:1187–1195, 1997. © 1997 Elsevier Science Inc.

**KEY WORDS.** oxidation; CYP3A2; CYP3A4; HIV protease inhibitor; intestinal metabolism

Many factors can influence the oral bioavailability of drugs. One of the most important factors is first-pass metabolism. Because of a unique anatomical arrangement of the intestine and liver, oral drugs have to pass through the intestine first and then the liver before reaching systemic circulation. For this reason, there is an increasing interest in studying intestinal and hepatic first-pass metabolism [1, 2]. It has been demonstrated that the expression of P450s $\dagger$  in the intestine is isoform-selective in rats and humans [2, 3], and P450 isoforms in the CYP3A subfamily are present in the intestine of both species [2–4]. Intestinal first-pass metabolism mediated by CYP3A has been shown to be clinically relevant with several drugs, such as cyclosporin A [5] and midazolam [6].

Indinavir (L-735,524, MK-0639, CRIVAN $\text{\textcircled{R}}$ ), *N*-(2(R)-hydroxy-1(S)-indanyl)-2(R)-phenylmethyl-4(S)-hydroxy-

5-(1-(4-(3-pyridylmethyl)-2(S)-*N'*-(*t*-butylcarboxamido)piperazinyl))pentanamide, is a potent ( $K_i = 0.41 \text{ nM}$ ) and highly selective inhibitor for HIV protease [7]. Pharmacokinetic studies revealed that oxidative metabolism is the major route of elimination for indinavir in rats and humans and the contribution of conjugation to the elimination is minimal ( $< 0.5\%$  of dose) [8, 9]. Our previous *in vivo* studies in rats have shown that indinavir is subject to a substantial hepatic first-pass effect, whereas an intestinal first-pass effect is minimal [9]. The purpose of this study was to investigate and compare the hepatic and intestinal metabolism of indinavir in rats and humans using liver and intestinal microsomes. In addition, attempts were made to predict hepatic and intestinal first-pass extraction ratios using *in vitro* metabolic data ( $V_{\max}/K_m$ ).

## MATERIALS AND METHODS

### Chemicals

Indinavir (MK-0639) and its carbon-14 form were synthesized at Merck Research Laboratories (West Point, PA). The carbon-14 label was incorporated at the carbonyl position (Figure 1) with a specific activity of 33.08 mCi/mg.

\* Corresponding author: Masato Chiba, Ph.D., WP44B-100, Department of Drug Metabolism, Merck Research Laboratories, West Point, PA 19486. Tel. (215) 652-0794; (215) 652-2410.

$\dagger$  Abbreviations: HIV, human immune deficiency virus; and P450, microsomal cytochrome P450.

Received 21 August 1996; accepted 7 November 1996.

The drug occasionally was purified according to the HPLC method described below. Dexamethasone, phenobarbital, testosterone, and diethyldithiocarbamate were purchased from the Sigma Chemical Co. (St. Louis, MO). Ketoconazole was obtained from Research Diagnostics Inc. (Flanders, NJ). Furafylline, sulfaphenazole and S-mephenytoin were purchased from the Gentest Corp. (Woburn, MA). Tolbutamide was obtained from Research Biochemical International (Natick, MA). Hydroxylated metabolites of testosterone at the 2 $\alpha$ -, 2 $\beta$ -, 6 $\beta$ -, 7 $\alpha$ -, 16 $\alpha$ -, and 16 $\beta$ -positions were obtained from Steraloids (Wilton, NH). All other reagents were of analytical grade.

#### **Liver and Intestinal (Jejunum) Microsomes from Human and Anti-Rat CYP3A1 Rabbit Polyclonal Antibody**

Microsomal fractions of human jejunum and liver were obtained from the Keystone Skin Bank (Exton, PA). The original liver microsome codes (age, sex) were HHM-0057 (15, M); 0059 (50, F); 0065 (46, F); 0071 (60, F); 0079 (40, M); and 0095 (63, F), where M and F represent male and female, respectively. Similarly, the original intestinal microsome codes (age, sex) were HJM-0001 (26, M); 0003 (41, M); and 0006 (21, M). All microsomes were obtained from Caucasian donors. Microsomes were used as supplied.

Rabbit polyclonal antibody prepared against rat CYP3A1 and pre-immune control IgG were obtained from Human Biologics Inc. (Phoenix, AZ). The immunoinhibitory potency for CYP3A1/2- and 3A4-catalyzed activities in rat and human liver microsomes, respectively, was checked by measuring testosterone 2 $\beta$ - and 6 $\beta$ -hydroxylation activities in the presence of different amounts of antibody. The preliminary studies revealed that the anti-rat CYP3A1 antibody showed a strong immunoinhibitory effect on testosterone 2 $\beta$ - and 6 $\beta$ -hydroxylation in both rat and human liver microsomes (data not shown).

#### **Animals and Microsomal Preparation**

Male adult (12-week-old) rats of the Sprague-Dawley strain were purchased from Harlan Industries (Indianapolis, IN). For induction studies, rats were pretreated with an oral dose of phenobarbital (80 mg/kg/day for 4 days) or dexamethasone (50 mg/kg/day for 4 days). All rats were killed 24 hr after the last treatment. The liver and intestine were excised quickly from the same animal and perfused with ice-cold 1.15% KCl (w/v). Hepatic microsomes were prepared by differential ultracentrifugation [10]. Microsomal final pellets were resuspended in 0.15 M Tris-HCl buffer (pH 7.4) and stored at -70° until used. Intestinal microsomal fractions were prepared from the upper segment (e.g. duodenum + upper jejunum) of control and pretreated rats according to a technique that yielded a high specific content of total CO-binding protein [11]. Microsomal protein was measured by the method of Lowry et al. [12], with bovine serum albumin as the standard.

#### **Indinavir Metabolism Assay**

The oxidative metabolism of indinavir was measured in a system consisting of an NADPH-generating system and microsomes according to the method specified below.

Preliminary experiments indicated that the total metabolism of indinavir was linear against incubation time for up to 25 min at 4 mg/mL protein in human and rat preparations, except for dexamethasone-induced rat liver where linearity was found up to 10 min at 0.5 mg/mL protein. The incubation mixture (final volume of 100  $\mu$ L in 0.15 M Tris-HCl buffer, pH 7.4) consisted of an NADPH-generating system [20 mM glucose-6-phosphate (G6P), 0.4 I.U. G6P dehydrogenase (G6PDH), 20 mM MgCl<sub>2</sub>], various concentrations of [<sup>14</sup>C]indinavir (0.2 to 5 or 10  $\mu$ M), and 4 mg/mL microsomes. For the competitive inhibition studies with quinine, quinidine, S-mephenytoin and ketoconazole, an appropriate concentration of inhibitor (up to 100  $\mu$ M) also was included in the reaction mixture. After a 5-min preincubation at 37°, the reaction was initiated by the addition of 10  $\mu$ L of 50 mM NADPH. For the inhibition study with furafylline and diethyldithiocarbamate, both mechanism-based inhibitors, a different concentration of inhibitor (up to 100  $\mu$ M) was preincubated with NADPH-fortified microsomes for 20 min at 37° prior to the addition of substrate. After the reaction started, the mixture was incubated for 5 or 20 min. The reaction was terminated by the addition of 300  $\mu$ L of ice-cold acetonitrile. The resultant mixture was mixed vigorously and centrifuged at 14,000 g for 4 min to precipitate protein. An aliquot of the supernatant (380  $\mu$ L) was transferred to a clean test tube and evaporated under nitrogen. The sample was reconstituted with 300  $\mu$ L H<sub>2</sub>O for injection onto the HPLC system described below. The recovery of total counts after the protein-precipitation procedure was found to be greater than 90%.

The designated amount of polyclonal anti-rat CYP3A1 rabbit antibody or pre-immune rabbit IgG was incubated with microsomes for 30 min at room temperature prior to adding the reaction mixture. The incubation mixture consisted of the same composition as described above, with the exception of the final microsomal concentration which was adjusted to 0.5 mg/mL. After the start of the reaction, the incubation was carried out for 40 min. The metabolism of indinavir was measured by the same protocol as described above.

Indinavir and its metabolites were measured by an HPLC system (Waters 600E System/717 WISP Autosampler, Milford, MA) equipped with a reverse-phase column (Supelcosil LC-18, 15 cm  $\times$  4.6 mm, 3  $\mu$ m). Mobile phase A consisted of 10 mM phosphate buffer (pH 5.2) and 5 mM hexyltriethylammonium phosphate. Mobile phase B consisted of acetonitrile. The following gradient system was used: 25% B to 30% B linearly over the first 40 min, isocratic 30% B for 15 min, and then 30% to 25% B for 5 min. The flow rate was 1 mL/min. Each biological sample was treated with a mixture of synthetic indinavir metabolites,

and elution from the column was monitored at 210 nm. The column eluent was collected by a fraction collector as follows: 1-min samples were collected for 9 min, 30-sec samples were collected between 9 and 31 min, and 2-min samples were collected up to 55 min. The  $^{14}\text{C}$ -radioactivity in the collected samples was measured with a liquid scintillation spectrophotometer (model LS-5000CE, Beckman Instruments, Fullerton, CA). The chromatographic peaks were assigned (based on the retention times of the corresponding standards) as follows (see Fig. 1): 2',3'-*trans*-dihydroxyindanylpiperidine *N*-oxide (M2), 2',3'-*trans*-dihydroxyindan (M3), pyridine *N*-oxide (M4a) and *p*-hydroxyphenylmethyl (M4b) analogs of indinavir, *N*-[2(S),3(S)-dihydroxy-1(S)-indanyl]-5-[2(S)-(1,1-dimethylethylaminocarbonyl) piperizin-1-yl]-4(S)-(hydroxy-2(R)-phenylmethylpentanamide (M5), and *N*-[2(R)-hydroxy-1(S)-indanyl]-5-[2(S)-(1,1-dimethylethylaminocarbonyl)piperizin-1-yl]-4(S)-hydroxy-2(R)-phenylmethyl pentanamide (M6). The recovery after HPLC analysis was calculated to be more than 90%, as determined by comparing the injected counts with the integrated counts in the eluted samples.

### Testosterone Hydroxylase Assay

P450-isoform specific hydroxylase assays of testosterone were performed using HPLC according to the following method specified below.

As incubation mixture (final volume of 250  $\mu\text{L}$  in 0.15 M Tris-HCl buffer, pH 7.4), containing an NADPH-generating system (G6P, 20 mM; G6PDH, 4 IU/mL;  $\text{MgCl}_2$ , 20 mM), 1 mg/mL microsomes, testosterone (100  $\mu\text{M}$  for the competitive inhibition study by indinavir; 12.5, 25, 50, and 100  $\mu\text{M}$  for examining the type of interaction between testosterone and indinavir), and various concentrations of indinavir, was preincubated for 5 min at 37°. Metabolism was initiated by the addition of NADPH at a final concentration of 1 mM. The reaction was conducted at 37° for 20 min and stopped by the addition of ice-cold ethyl acetate (1.0 mL). Then an internal standard (50  $\mu\text{L}$  of 20  $\mu\text{M}$  cortisone) was added to each sample, followed by an additional 1.5 mL of ethyl acetate to extract metabolites. The resulting mixture was vortex-mixed, and the ethyl acetate layer was separated by centrifugation, followed by evaporation to dryness under nitrogen. The residue was reconstituted in 150  $\mu\text{L}$  of 20% methanol in water.

An HPLC assay was performed on a Supelco LC-18 column (5  $\mu\text{m}$ , 4.6 mm  $\times$  15 cm) with a Spectra-Physics HPLC system (Fremont, CA). The HPLC method involved isocratic elution for 3.5 min with an 83:17 (v/v) mixture of 30% methanol in water (mobile phase A) and 10% acetonitrile in methanol (mobile phase B) at a flow rate of 1.0 mL/min. Both mobile phases were adjusted to pH 4.5 with glacial acetic acid. Then a linear gradient was run until 10 min, when the proportion of mobile phase A was decreased from 83 to 70%. Mobile phase A remained at 70% until 25 min, after which it was further decreased to 50% at 30 min.

Then mobile phase A was returned to 83% at 35 min. The metabolites were monitored at 240 nm.

### Scale up of *in vitro* $V_{\text{max}}/K_m$

To extrapolate the *in vitro*  $V_{\text{max}}/K_m$  ( $\mu\text{L}/\text{min}/\text{mg}$  protein) to the *in vivo* intrinsic clearance for predicting first-pass elimination in the liver and intestine, we used the following parameters and equations. The *in vitro* value was extrapolated to the *in vivo* intrinsic clearance ( $CL_{\text{int, in vivo}}$ , mL/min/kg body weight) according to the equation:

$$CL_{\text{int, in vivo}} = (V_{\text{max}}/K_m) \cdot M \cdot \text{OW}/f_u \quad (1)$$

where  $M$ ,  $\text{OW}$ , and  $f_u$  represent the microsomal yield (mg/g tissue), liver or intestine weight (g/kg body weight), and the unbound fraction of indinavir in the microsomal reaction mixture, respectively. The microsomal protein yield ( $M$ ) has been reported to be about 3 and 50 mg/g organ for the intestine [13] and liver [14], respectively, and we assumed the same protein contents between human and rat. The liver weight was estimated from the allometric relationship: liver weight =  $0.037 W^{0.85}$  [where  $W$  is the body weight (kg)] [15]. The liver weight (normalized by kg body weight) used in the calculation was 45 and 20 g/kg for rats and humans, respectively. The intestinal weights for rats and humans were taken from literature [16]: 45 and 30 g/kg for rats and humans, respectively. To correct the  $K_m$  value for unbound drug concentration, we measured the unbound fraction of indinavir in the microsomal reaction mixture ( $f_u$ ). Indinavir was added to the reaction mixture described above to yield a final concentration of 5  $\mu\text{M}$ . Following incubation of the reaction mixture without NADPH at 37° for 20 min, an aliquot of the mixture (1 mL) was transferred to a Centrifree tube (Amicon Co., Danvers, MA) and centrifuged at 1500  $g$  for 15 min at 37°. The unbound fraction was estimated directly from the ratio of drug concentration in the ultrafiltrate to that in the original reaction mixture sample. No significant difference was observed in the unbound fraction between the liver and intestine in either species.

The hepatic clearance ( $CL_H$ ) and the hepatic extraction ratio ( $E$ ) were determined according to the "well-stirred" model as follows [17]:

$$CL_H = Q \cdot E = \frac{Q \cdot f_B \cdot CL_{\text{int, in vivo}}}{Q + f_B \cdot CL_{\text{int, in vivo}}} \quad (2)$$

where  $Q$  is the hepatic blood flow and  $f_B$  is the unbound fraction of indinavir in the blood. The hepatic blood flow rates used in the calculation of  $CL_H$  and  $E$  are 65 mL/min/kg for rats and 20 mL/min/kg for humans [15]. The unbound fraction of indinavir in the blood for rats and humans was

taken from the literature [9]. For the intestine, the same equation was used to predict clearance and first-pass elimination. The mucosal blood flow rate was used in the equation instead of the total intestinal blood flow rate as proposed by Klippert *et al.* [18]: the mucosal blood flow rate for rats was taken from the literature (15 mL/min/kg [19]). The same ratio of mucosal to hepatic blood flow rate as used for rats was employed to calculate the human mucosal blood flow rate [i.e.  $20 \times (15/65) = 4.6$  mL/min/kg].

## RESULTS

### Hepatic and Intestinal Metabolism of Indinavir

In a clinical study, seven prominent metabolites were isolated from human urine and characterized by NMR, MS, and/or chromatographic comparisons with authentic standards [20]. The major metabolic pathways were identified in human as (a) glucuronidation at the pyridine nitrogen to yield a quaternized ammonium conjugate (M1), (b) pyridine N-oxidation (M2 and M4a), (c) *para*-hydroxylation of the phenylmethyl group (M4b), (d) 3'-hydroxylation of the indan moiety (M2, M3, and M5), and (e) N-depyridomethylation (M5 and M6) (Fig. 1). All oxidative metabolites observed *in vivo* also were formed in NADPH-fortified liver and intestinal microsomes. N-Dealkylation was quantitatively the most important biotransformation pathway for indinavir; more than 50% of the drug was

converted to N-dealkylated metabolites, M5 and M6 (data not shown). Because of the formation of the secondary oxidative metabolites (M2, M5, and M6) during incubation, kinetic studies were conducted to estimate apparent  $K_m$  and  $V_{max}$  values for the formation of total metabolites ( $M2 + M3 + M4a + M4b + M5 + M6$ ). The apparent  $K_m$  and  $V_{max}$  values are summarized in Table 1. The  $K_m$  values in the liver microsomes of both rats and humans were approximately 2-fold smaller than those obtained from the intestine of the corresponding species (Table 1). The low  $K_m$  values, ranging from 1.0 to 2.5  $\mu$ M, suggest a high affinity of indinavir for the metabolizing enzymes. When the enzyme activities were expressed per milligram of microsomal protein, the average of  $V_{max}$  values obtained from rat liver microsomes was approximately 5-fold larger than that from the intestinal microsomes, whereas there was no significant difference in  $V_{max}$  between the liver and intestine in humans. The values for  $V_{max}/K_m$  of both species were 2- to 8-fold higher in the liver than in the intestine (Table 1).

### Identification of P450 Isoform(s) Responsible for Hepatic and Intestinal Indinavir Metabolism

In our previous study with human liver microsomes [21], we demonstrated that all oxidative metabolic pathways of indinavir were mediated by CYP3A4. This conclusion was based on the results of five *in vitro* approaches proposed by

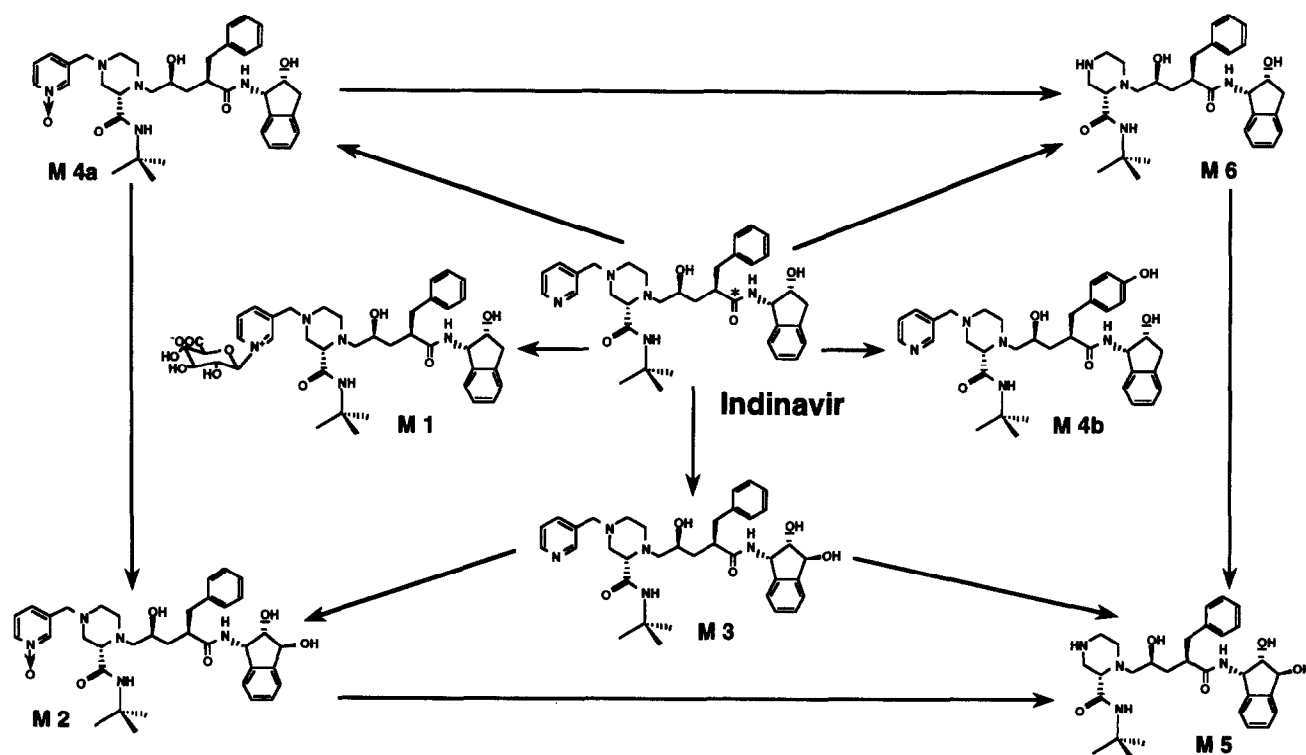


FIG. 1. Proposed metabolic pathway of indinavir in humans. Metabolite structures have been identified in human urine and feces samples [20].

**TABLE 1. Kinetics of liver and intestine microsomal (total) metabolism of indinavir in rat and human\***

Species	Organ	$K_m$ ( $\mu\text{M}$ )	$V_{\text{max}}$ ( $\text{pmol/min/mg}$ )	$V_{\text{max}}/K_m$ ( $\mu\text{L/min/mg}$ )
Rat†	Liver	1.03 (0.07)	57.4 (9.9)	55.8 (7.9)
	Intestine	1.68 (0.06)	11.3 (1.9)	6.74 (1.21)
Human	Liver‡	1.30 (0.25)	22.9 (20.5)	16.5 (13.3)
	Intestine§	2.51 (0.77)	17.4 (3.4)	7.74 (4.03)

\* Total metabolic rate at each substrate concentration was generated by summing formation rates. The obtained Michaelis-Menten-type saturable curve then was analyzed for  $K_m$  and  $V_{\text{max}}$  values.

† Data represent the average of results obtained from three preparations. Numbers in parentheses represent the SD.

‡ Data represent the average of results obtained from six different human liver microsomes. Numbers in parentheses represent the SD.

§ Data represent the average of results obtained from three different human intestine (jejunum) microsomes. Numbers in parentheses represent the SD.

Guengerich and Shimada [22], namely: (1) chemical inhibition, (2) immunochemical inhibition, (3) metabolism by cDNA-expressed human P450 enzymes, (4) correlation analysis, and (5) competitive inhibition of marker activities. To determine which P450 isoform(s) is responsible for the oxidative metabolism of indinavir in rat hepatic and intestinal microsomes and human intestinal microsomes, we examined the effect of ketoconazole and an anti-rat CYP3A1 antibody on indinavir metabolism. For comparison, the effects of ketoconazole and an anti-rat CYP3A1 antibody on indinavir metabolism in human hepatic microsomes also were studied.

Ketoconazole, a CYP3A-selective inhibitor, strongly inhibited indinavir metabolism in both hepatic and intestinal microsomes of rats and humans in a concentration-dependent manner (Fig. 2). Other chemical inhibitors (i.e. furafylline, quinidine, sulfaphenazole, diethyldithiocarbamate, and *S*-mephenytoin for human microsomes; quinidine and furafylline for rat microsomes) had little effect on either hepatic and intestinal metabolism of indinavir (data not shown). These results suggest the possible involvement of CYP3A isoforms in both liver and intestinal microsomes of rats and humans. Consistent with this, an anti-rat CYP3A1 antibody, which shows a cross-reactive inhibition

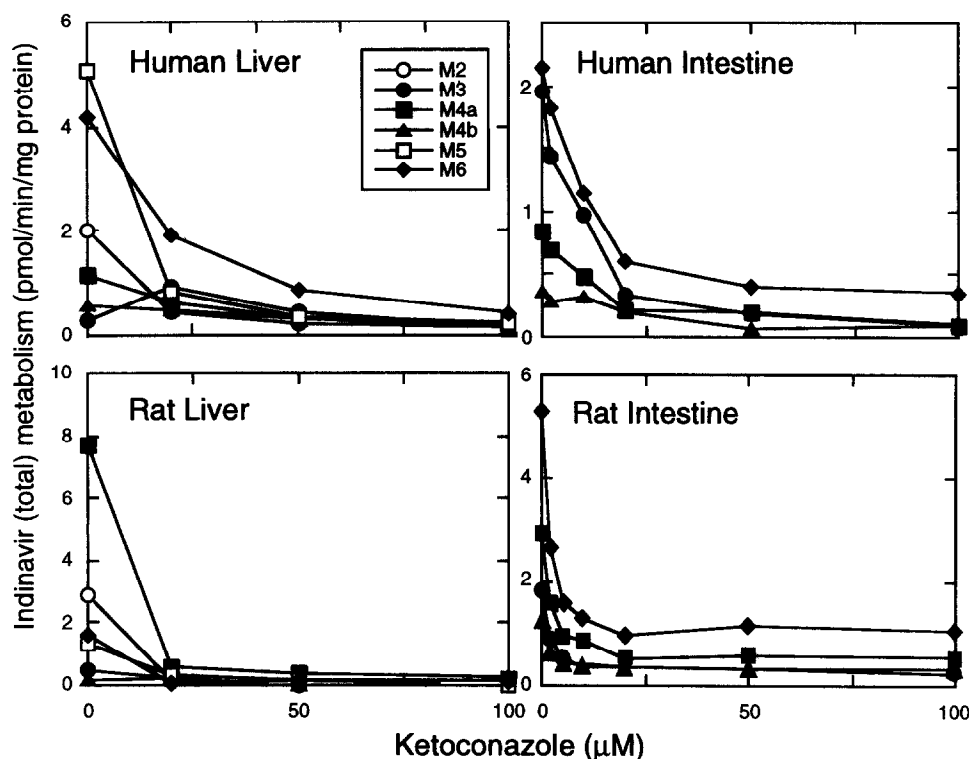
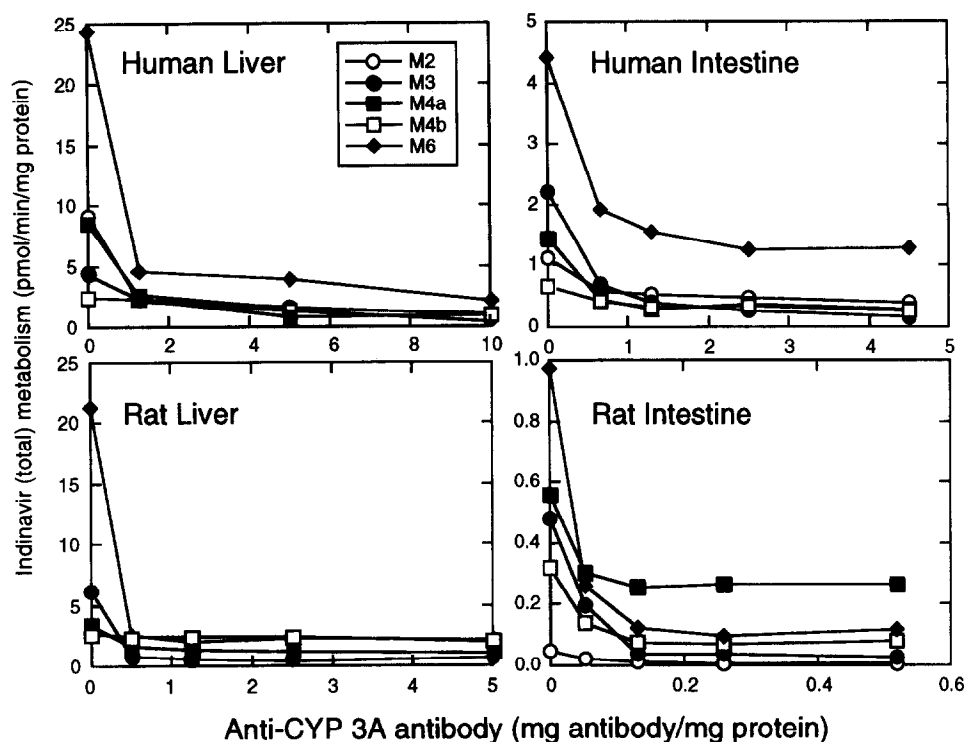


**FIG. 2.** Effect of ketoconazole on indinavir metabolism in human and rat microsomes. Secondary metabolites M2 and M5 were not clearly formed in the intestinal microsomes under these conditions. Microsomal fraction pooled from three individuals was used.

FIG. 3. Effect of anti-CYP3A1 antibody on indinavir metabolism in human and rat microsomes. Pre-immune IgG had little effect on indinavir metabolism (data not shown). Microsomal fraction pooled from three individuals was used.



of human CYP3A4-dependent testosterone 6 $\beta$ -hydroxylation, markedly inhibited all hepatic and intestinal microsomal oxidations of indinavir in both species (Fig. 3). Furthermore, oral treatment of rats with dexametha-

sone, a potent CYP3A inducer, increased the formation of all metabolites of indinavir in both rat liver and intestinal microsomes by a factor of 7 and 3, respectively (Fig. 4). Phenobarbital induced hepatic metabolism of indinavir ap-

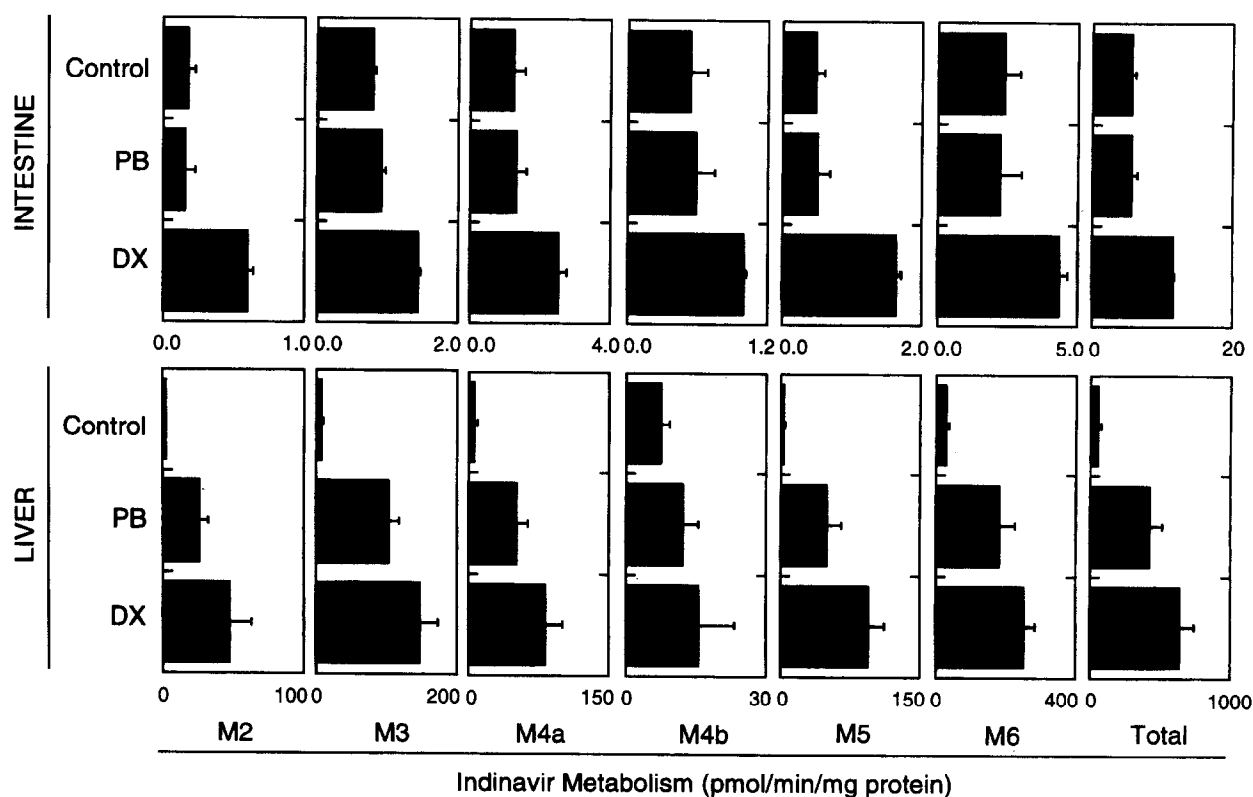


FIG. 4. Indinavir metabolism in induced rat liver and intestinal microsomes. Microsomes were obtained from rats pretreated with DX (50 mg/kg/day dexamethasone p.o. for 4 days) or PB (80 mg/kg/day phenobarbital p.o. for 4 days). Control microsomes were obtained from untreated rats. Data represent the means  $\pm$  SD of three different preparations.

proximately 2-fold, but had little effect on intestinal indinavir metabolism. These results supported the fact that a CYP3A isoform(s) is responsible for indinavir metabolism in rats.

Competitive inhibition studies of CYP3A-selective marker activity further confirmed that the major oxidative metabolic pathways were catalyzed mainly by a CYP3A isoform(s) in rat and human liver microsomes. Indinavir strongly inhibited testosterone 2 $\beta$ -/6 $\beta$ -hydroxylase activities in both rat and human liver microsomes in a concentration-dependent manner (Fig. 5). Kinetic analysis (Lineweaver-Burk plots, Fig. 6A; Dixon plots, Fig. 6B) revealed that indinavir is a potent competitive inhibitor on CYP3A isoforms in rat liver microsomes, with a  $K_i$  value of approximately 0.7  $\mu$ M. Similarly, the competitive inhibition of indinavir on 6 $\beta$ -hydroxylase activity also was observed in human liver microsomes, with a  $K_i$  value of 0.5  $\mu$ M. The inhibition constant values were comparable to those of the apparent  $K_m$  values for total indinavir metabolism in rat and human liver microsomes ( $\sim$ 1.0  $\mu$ M) (Table 1).

## DISCUSSION

In both rats and humans, indinavir was metabolized much more rapidly by liver microsomes than by intestinal microsomes. The  $V_{max}/K_m$  values ( $\mu$ L/min/mg microsomal protein) obtained from hepatic microsomes were 8-fold higher than those from intestinal microsomes for the rat, and 2-fold higher for human (Table 1). When the *in vitro*  $V_{max}/K_m$  values were scaled up to *in vivo* intrinsic clearance (mL/

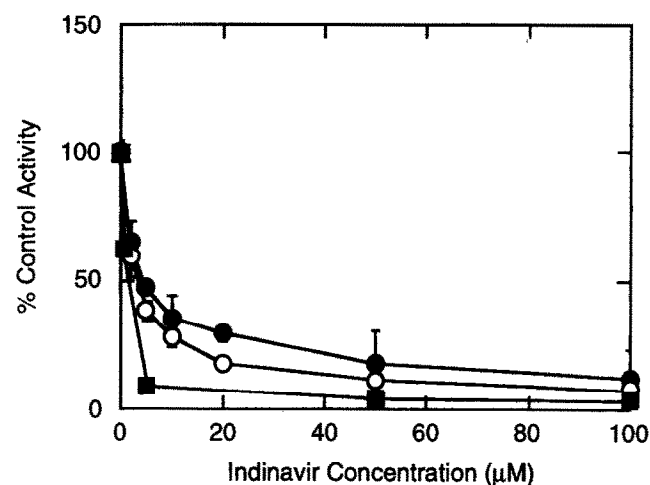


FIG. 5. Effect of indinavir on testosterone hydroxylase activities in rat and human liver microsomes. Hydroxylase activities of testosterone at the 2 $\beta$ - (●) and 6 $\beta$ - (○) positions in rat liver microsomes and the 6 $\beta$ -position in human liver microsomes (■) were measured. Data represent means  $\pm$  SD of three different preparations for rats. Metabolic activities at 0  $\mu$ M indinavir were:  $0.017 \pm 0.002$  nmol/min/mg protein for 2 $\beta$ -hydroxylase in rats ( $N = 3$ , mean  $\pm$  SD);  $0.222 \pm 0.018$  nmol/min/mg protein for 6 $\beta$ -hydroxylase in rats ( $N = 3$ , mean  $\pm$  SD); and  $0.105$  nmol/min/mg protein for 6 $\beta$ -hydroxylase in human ( $N = 1$ ).

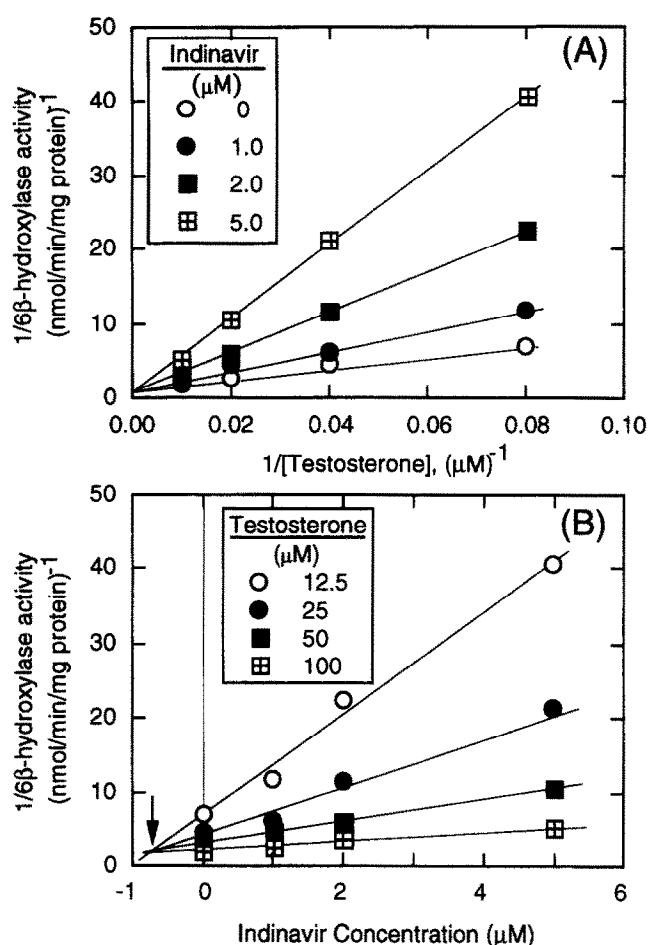


FIG. 6. Inhibition kinetics of testosterone 6 $\beta$ -hydroxylase activity by indinavir in rat liver microsomes. Lineweaver-Burk plots (A) revealed a competitive interaction between indinavir metabolism and testosterone 6 $\beta$ -hydroxylation. The inhibition constant was graphically estimated to be 0.7  $\mu$ M based on the Dixon plots (B).

min/kg body weight), the differences in metabolizing capacity between the liver and intestine became more significant (i.e. 200-fold for the rat and 50-fold for the human) due to the big difference in the total content of microsomal protein between the two tissues; microsomal yield in the liver has been reported to be  $\sim$ 50 mg/g liver [14], while only 3 mg/g organ for the intestine [13].

Hepatic and intestinal first-pass effects have been predicted successfully based on *in vitro* metabolic data [18]. With the same approach, we estimated the hepatic and intestinal first-pass extraction ratio using *in vitro*  $V_{max}/K_m$  data. The estimations were carried out using the well-stirred model, which incorporates the mucosal blood flow rate instead of the total intestinal flow rate. In rats, hepatic and intestinal first-pass effects were estimated to be 42 and 2%, respectively (Table 2). These values agreed reasonably well with the *in vivo* observations in rats [9]. The hepatic first-pass metabolism of indinavir in rats was estimated to be 67% when drug concentrations in the systemic blood during portal and femoral vein infusion were compared under the steady-state condition. On the other hand, the intesti-

TABLE 2. Prediction of hepatic and intestinal first-pass effects of indinavir based on *in vitro* kinetic parameters

Species	Organ	$V_{\max}/K_m^*$ ( $\mu\text{L}/\text{min}/\text{mg}$ )	$\text{CL}_{\text{int, in vivo}}^\dagger$ ( $\text{mL}/\text{min}/\text{kg}$ )	Blood flow rate $^\ddagger$ ( $\text{mL}/\text{min}/\text{kg}$ )	$f_B^\S$	$\text{CL}_{\text{organ}}^\parallel$ ( $\text{mL}/\text{min}/\text{kg}$ )	$E_{\text{organ}}^\P$ (%)
Rat	Liver	69.7	159	65	0.30	27.5	42.3
	Intestine	8.41	0.808	15	0.30	0.326	2.17
Human	Liver	18.6	18.2	20	0.39	5.23	26.1
	Intestine	8.71	0.373	4.6	0.39	0.287	6.23

\* Values were calculated from:  $(V_{\max}/K_m)/f_u$ , where  $V_{\max}/K_m$  was taken from Table 1 and  $f_u$  is an unbound fraction of indinavir in the microsomal reaction mixture (0.801 for rat microsomes, 0.889 for human microsomes).

$^\dagger \text{CL}_{\text{int, in vivo}} = (V_{\max}/K_m) \cdot (\text{microsomal content, mg/g organ}) \cdot (\text{organ weight, g/kg body weight})$ . Microsomal contents were assumed to be 3 and 50 mg/g organ for intestine and liver, respectively [13, 14]. Organ weights for rat and human liver were 45 and 20 g/kg, respectively; the values for rat and human intestine were 45 and 30 g/kg, respectively (see Materials and Methods).

$^\ddagger$  Liver blood flow rates were taken from the literature [15]. Mucosal blood flow was used instead of total intestinal blood flow to predict a flow rate for the "metabolizing compartment" in the intestine as proposed by Klippert et al. [18]. Human mucosal blood flow rate was calculated by using the blood flow rate ratio of intestine to liver of rats [i.e.  $20 \times (15/65) = 4.6 \text{ mL}/\text{min}/\text{kg}$ ].

$^\S$  Taken from Ref. 9.

$^\parallel \text{CL}_{\text{organ}} = \frac{Q \cdot f_B \cdot \text{CL}_{\text{int, in vivo}}}{Q + f_B \cdot \text{CL}_{\text{int, in vivo}}}$  where  $Q$  represents organ blood flow rate.

$^\P E_{\text{organ}} = \frac{f_B \cdot \text{CL}_{\text{int, in vivo}}}{Q + f_B \cdot \text{CL}_{\text{int, in vivo}}}$

nal first-pass elimination was minimal (< 10%). More than 90% of the radioactivity collected in the mesenteric blood from the *in situ* isolated intestinal loop preparation was unchanged drug. With the same *in vitro* approach, we predicted that the hepatic first-pass metabolism of indinavir was 26%, while the contribution of the intestine was limited ( $E = 6\%$ ) in human (Table 2).

In summary, *in vitro* kinetic studies revealed that the liver plays a much greater role in the first-pass metabolism of indinavir than the intestine after oral administration. Using *in vitro* metabolic data, hepatic and intestinal first-pass metabolism was predicted reasonably well in rats. Based on *in vitro* intrinsic clearance of the human hepatic and intestinal microsomes, a significant first-pass metabolism was predicted in the liver, while the metabolic elimination in the intestine would be limited.

## References

- Kaminsky LS and Fasco MJ, Small intestinal cytochrome P450. *Crit Rev Toxicol* 21: 407–422, 1992.
- Zhang Q-Y, Wikoff J, Dunbar D and Kaminsky L, Characterization of rat small intestinal cytochrome P-450 composition and inducibility. *Drug Metab Dispos* 24: 322–328, 1996.
- de Waziers I, Cugnenc PH, Yang CS, Leroux J-P and Beaune PH, Cytochrome P450 isoenzymes, epoxide hydrolase and glutathione transferases in rat and human hepatic and extrahepatic tissues. *J Pharmacol Exp Ther* 253: 387–394, 1990.
- Kolars JC, Schmiedlin-Ren P, Dobbins WO III, Schuetz J, Wrighton SA and Watkins PB, Heterogeneity of cytochrome P450III $\alpha$  expression in rat gut epithelia. *Gastroenterology* 102: 1186–1198, 1992.
- Hebert MF, Roberts JP, Prueksaritanont T and Benet LZ, Bioavailability of cyclosporine with concomitant rifampin administration is markedly less than predicted by hepatic enzyme induction. *Clin Pharmacol Ther* 52: 453–457, 1992.
- Paine MF, Shen DD, Kunze KL, Perkins JD and Thummel KE, Intestinal metabolism of midazolam by the anhepatic transplant patient. *ISSX Proc* 8: 298, 1995.
- Vacca JP, Dorsey BD, Schleif WA, Levin RB, McDaniel SL, Darke PL, Zugay J, Quintero JC, Blahy OM, Roth E, Sardana VV, Schlabach AJ, Graham PI, Condra JH, Gotlib L, Holloway MK, Lin JH, Chen I-W, Vastag K, Ostovic D, Anderson PS, Emini EA and Huff JR, L-735,524: An orally bioavailable human immunodeficiency virus type 1 protease inhibitor. *Proc Natl Acad Sci USA* 91: 4096–4100, 1994.
- Lin JH, Chen I-W, Vastag KJ and Ostovic D, pH-Dependent oral absorption of L-735,524, a potent HIV protease inhibitor, in rats and dogs. *Drug Metab Dispos* 23: 730–735, 1995.
- Lin JH, Chiba M, Balani SK, Chen I-W, Kwei GY-S, Vastag KJ and Nishime JA, Species differences in the pharmacokinetics and metabolism of indinavir, a potent HIV protease inhibitor. *Drug Metab Dispos* 24: 1111–1120, 1996.
- Omura T and Sato R, The carbon-monoxide binding pigment of liver microsomes. *J Biol Chem* 239: 2370–2378, 1964.
- Bonkovsky HL, Hauri H-P, Marti U, Gasser R and Meyer UA, Cytochrome P450 of small intestinal epithelial cells: Immunochemical characterization of the increase in cytochrome P450 caused by phenobarbital. *Gastroenterology* 88: 458–467, 1985.
- Lowry OH, Rosebrough NJ, Farr AL and Randall RJ, Protein measurement with the Folin phenol reagent. *J Biol Chem* 193: 265–275, 1951.
- Borm P, Frankhuijzen-Sierevogel A and Noordhoek J, Time and dose dependence of 3-methylcholanthrene-induced metabolism in rat intestinal mucosal cells and microsomes. *Biochem Pharmacol* 31: 3707–3710, 1982.
- Houston JB, Utility of *in vitro* drug metabolism data in prediction of *in vivo* metabolic clearance. *Biochem Pharmacol* 47: 1469–1479, 1994.
- Boxenbaum H, Interspecies variation in liver weight, hepatic blood flow and antipyrine intrinsic clearance in extrapolation of data to benzodiazepines and phenytoin. *J Pharmacokinet Biopharm* 8: 165–176, 1980.
- Gerlowski LE and Jain RK, Physiologically based pharmacokinetic modeling: Principles and applications. *J Pharma Sci* 72: 1103–1127, 1983.
- Pang KS and Rowland M, Hepatic clearance of drugs. I. Theoretical consideration of a "well-stirred" model and a "parallel tube" model. Influence of hepatic blood flow, plasma and blood cell binding, and the hepatocellular activity on hepatic drug clearance. *J Pharmacokinet Biopharm* 5: 625–653, 1977.



18. Klippert P, Borm P and Noordhoek J, Prediction of intestinal first-pass effect of phenacetin in the rat from enzyme kinetic data—Correlation with *in vivo* data using mucosal blood flow. *Biochem Pharmacol* **31**: 2545–2548, 1982.
19. Bohlen HG, Henrich H, Gore RW and Johnson PC, Intestinal muscle and mucosal blood flow during direct sympathetic stimulation. *Am J Physiol* **235**: H40–H45, 1978.
20. Balani SK, Arison BH, Mathai L, Kauffman L, Miller RR, Stearns RA, Chen I-W and Lin JH, Metabolites of L-735,524, a potent HIV-1 protease inhibitor, in human urine. *Drug Metab Dispos* **23**: 266–270, 1995.
21. Chiba M, Hensleigh M, Nishime JA, Balani SK and Lin JH, Role of cytochrome P-450 3A4 in human metabolism of MK-639, a potent HIV protease inhibitor. *Drug Metab Dispos* **24**: 307–314, 1996.
22. Guengerich FP and Shimada T, Oxidation of toxic and carcinogenic chemicals by human cytochrome P-450 enzymes. *Chem Res Toxicol* **4**: 391–407, 1991.